THE ASTROPHYSICAL JOURNAL, 538:581–593, 2000 August 1

THE NARROW-LINE REGION OF NARROW-LINE SEYFERT 1 GALAXIES[1]

A. RODRÍGUEZ-ARDILA[2,3,4]
Departamento de Astronomia—UFRGS. CP 15051, Porto Alegre, Brazil

LUC BINETTE
Instituto de Astronomía, UNAM, Ap. 70-264, 04510 D.F., Mexico

MIRIANI G. PASTORIZA
Departamento de Astronomia—UFRGS. CP 15051, Porto Alegre, Brazil

AND

CARLOS J. DONZELLI[2]
IATE, Observatorio Astronómico, Universidad Nacional de Córdoba Laprida 854, 5000, Córdoba, Argentina
Received 1999 September 20; accepted 2000 March 3

ABSTRACT

This work studies the optical emission-line properties and physical conditions of the narrow-line region (NLR) of seven narrow-line Seyfert 1 galaxies (NLS1's) for which high signal-to-noise ratio spectroscopic observations were available. The resolution is 340 km s^{-1} (at Hα) over the wavelength interval 3700–9500 Å, enabling us to separate the broad and narrow components of the permitted emission lines. Our results show that the flux carried out by the narrow component of Hβ is, on average, 50% of the total line flux. As a result, the [O III] λ5007/Hβ ratio emitted in the NLR varies from 1 to 5, instead of the universally adopted value of 10. This has strong implications for the required spectral energy distribution that ionizes the NLR gas. Photoionization models that consider a NLR composed of a combination of matter-bounded and ionization-bounded clouds are successful at explaining the low [O III] λ5007/Hβ ratio and the weakness of low-ionization lines of NLS1's. Variation of the relative proportion of these two type of clouds nicely reproduces the dispersion of narrow-line ratios found among the NLS1 sample. Assuming similar physical model parameters of both NLS1's and the normal Seyfert 1 galaxy NGC 5548, we show that the observed differences of emission-line ratios between these two groups of galaxies can be explained, to a first approximation, in terms of the shape of the input ionizing continuum. Narrow emission-line ratios of NLS1's are better reproduced by a steep power-law continuum in the EUV–soft X-ray region, with spectral index $\alpha \sim -2$. Flatter spectral indices ($\alpha \sim -1.5$) match the observed line ratios of NGC 5548 but are unable to provide a good match to the NLS1 ratios. This result is consistent with *ROSAT* observations of NLS1's, which show that these objects are characterized by steeper power-law indices than those of Seyfert 1 galaxies with strong broad optical lines.

Subject headings: galaxies: nuclei — galaxies: Seyfert — X-rays: galaxies

1. INTRODUCTION

Narrow-line Seyfert 1 galaxies (hereafter NLS1's) are a peculiar group of AGNs in which the permitted optical lines show full width half-maximum (FWHM) not exceeding 2000 km s^{-1}, the [O III] λ5007/Hβ ratio is less than 3, and the UV–visual spectrum is usually very rich in high-ionization lines and Fe II emission multiplets. In the soft X-ray band, NLS1's have generally much steeper continuum slopes and rapid variability (Boller, Brandt, & Fink 1996, hereafter BBF96). Recently, Leighly (1999) found that the hard X-ray photon index is significantly steeper in NLS1's compared with that of normal Seyfert 1's and that soft excess emission appears considerably more frequently in NLS1's than in Seyfert 1 galaxies with broad optical lines.

It is not known at present the origin of the narrowness of broad permitted lines in NLS1's. Osterbrock & Pogge (1985), Ulvestad, Antonucchi, & Goodrich (1985), and Stephens (1989) suggest that if the velocities in the BLR of Seyfert 1's were largely confined to a plane, the NLS1 galaxies could be understood as cases in which the line of sight is nearly perpendicular to this plane. BBF96 state, on the other hand, that if the gravitational force from the central black hole is the dominant cause of the motions of Seyfert BLR clouds, narrower optical emission lines will result from smaller black hole masses provided the characteristics BLR distance from the central source does not change strongly with black hole masses.

However, Rodríguez-Pascual, Mass-Hesse, & Santos-Lléo (1997) report the detection in NLS1 galaxies of broad components with FWHM around 5000 km s^{-1} for the high-ionization UV permitted lines such as Lyα, C IV λ1550, and He II λ1640. This result indicates that gas moving at velocities comparable to those found in typical Seyfert 1 galaxies does indeed exist in NLS1's. In the optical region, they found "broad" components with FWHM less than 3000 km s^{-1}, narrower than the broadest UV component in the same objects. Nonetheless, deblending the optical permitted lines in NLS1's is difficult because no transition between the narrow and broad components is observed.

[1] Based on observations made at CASLEO. Complejo Astronómico El Leoncito (CASLEO) is operated under agreement between the Consejo Nacional de Investigaciones Científicas y técnicas de la República Argentina and the National Universities of La Plata, Córdoba and San Juán.

[2] Visiting Astronomer at CASLEO Observatory.

[3] CNPq Fellow.

[4] Present address: Observatorio Astronómico Nacional, Universidad Nacional de Colombia, Santafé de Bogotá, Colombia.

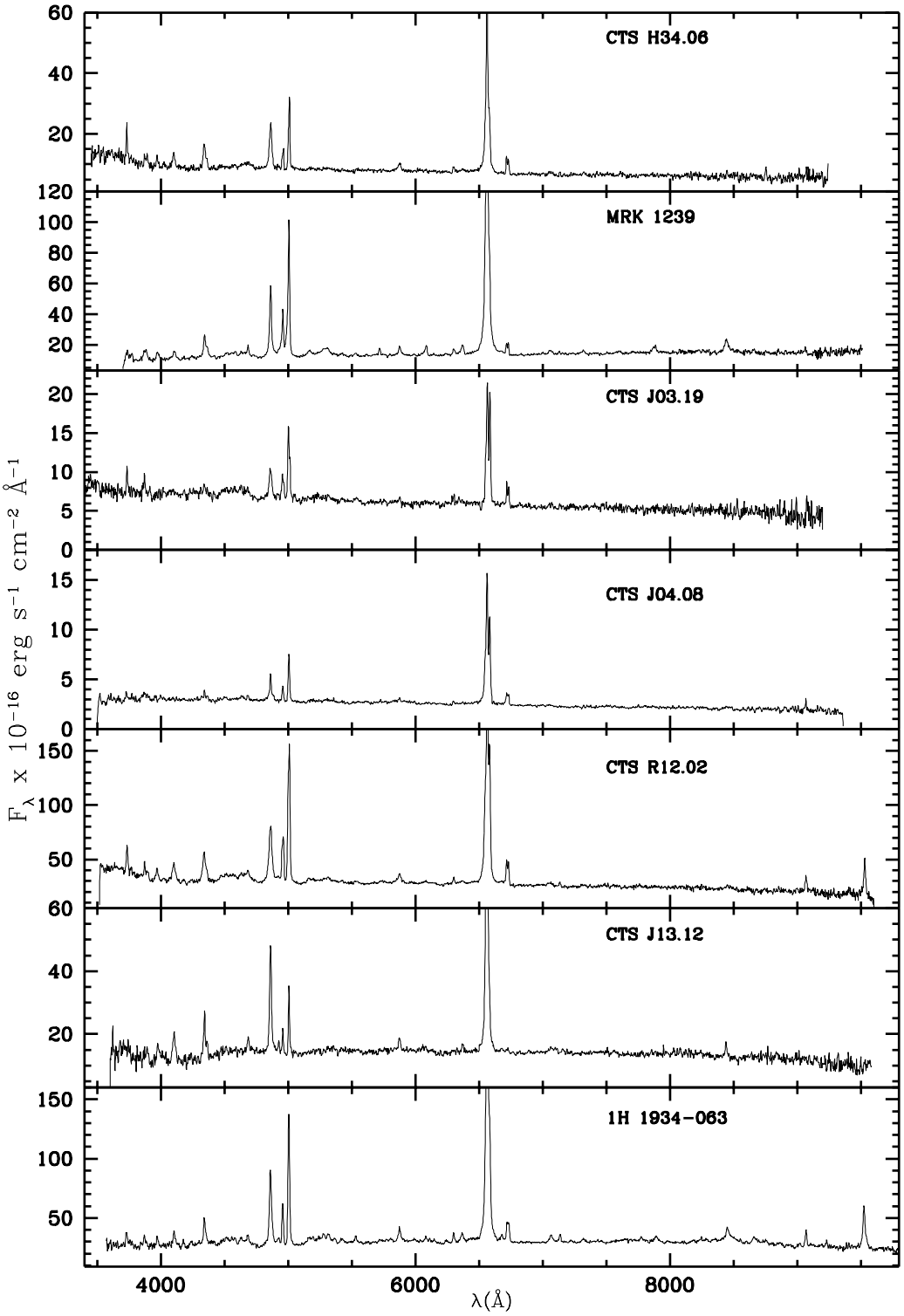

FIG. 1.—Sample of NLS1 galaxy spectra used in this work

This shortcoming has strong influences in, for example, the analysis of the narrow-line region (NLR) owing to the large uncertainties in determining the fraction of Hα and Hβ that originates from low-ionization material.

Up to now, most studies of the NLR in NLS1's assume that the flux emitted by the narrow Hβ equals 10% of the flux of [O III] λ5007 (Osterbrock & Pogge 1985; Leighly 1999). This assumption is based on the results obtained from Seyfert 2 and intermediate Seyfert 1 galaxies (e.g., Koski 1978; Cohen 1983). But in recent years, growing observational evidence points out to the existence of differences between the NLR of normal Syefert 1 and Seyfert 2 galaxies (Schmitt & Kinney 1996; Schmitt 1998), making the above assumption highly uncertain. In addition, fixing the [O III] λ5007/Hβ ratio to 10 implies ignoring the large scatter in the value of this ratio observed in normal Seyfert 1's (2 to 19; see, for example, Rodríguez-Ardila, Pastoriza, & Donzelli 2000, hereafter Paper I) and overlook the influ-

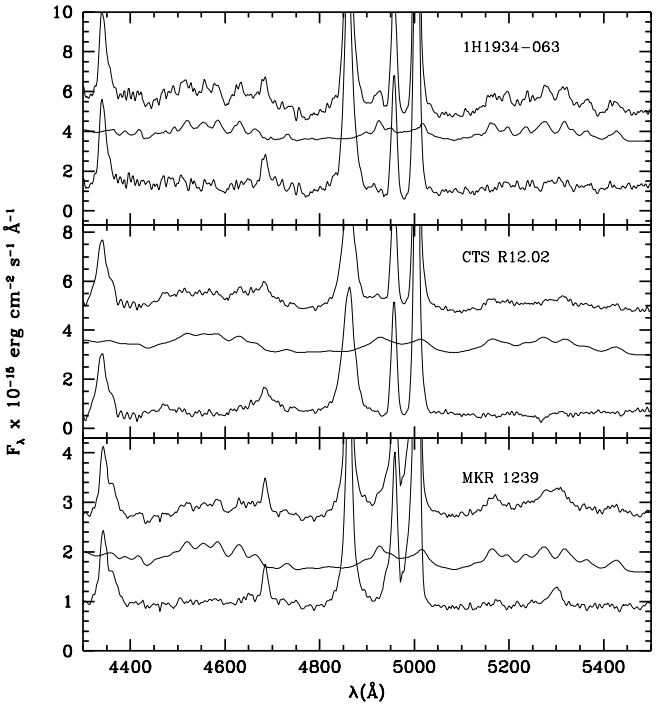

FIG. 2.—Example of the Fe II subtraction procedure carried out to the NLS1 galaxies 1H 1934−063 (*top panel*), CTS R12.02 (*middle panel*), and Mrk 1239 (*lower panel*). In each panel from top to bottom are the observed spectrum with the Fe II emission, the Fe II template that best matches this emission, and the residual Seyfert spectrum after subtracting the Fe II contribution. The spectra have been displaced by a constant factor for visualization purposes. In the residual spectrum note the flat continuum at both sides of Hβ and the appearance of the He II λ4686 line not clearly seen in the contaminated spectrum.

ences that this ratio could have in the energetics and physical conditions of the NLR of these objects.

For the above reason, the main purpose of this paper is to seek additional constraints in order to estimate the actual contribution of the narrow Hβ flux to the total Hβ emission line and study the implications that the newly adopted values could have on narrow-line ratios and the physics of the NLR of NLS1's.

The present work is organized as follows. In § 2 we describe the sample of NLS1's used in this paper. Section 3 presents the decomposition into narrow and broad components carried out in the Balmer lines of the NLS1 galaxies. Photoionization models that successfully reproduce the observed line ratios of NLS1's are presented in § 4. A discussion of the main results appears in § 5, and the conclusions are presented in § 6.

2. OBSERVATIONS

Long-slit spectroscopic observations of seven NLS1 galaxies covering the spectral region 3700–9500 Å were obtained with the 2.15 m telescope of the Complejo Astronomico El Leoncito (CASLEO) using a TEK 1024 × 1024 CCD detector and a REOSC spectrograph. Two gratings of 300 line mm^{-1} with blaze angles near 5500 and 8000 Å, respectively, were used in order to cover fully the spectral interval 3700–9500 Å. The spatial scale of this setup is 0.″95 pixel^{-1}, with an instrumental resolution of 7 Å FWHM. A slit width of 2.″5 oriented in the east-west direction and crossing the center of the galaxies was employed. The galaxies and standard stars were observed near the zenith (air masses < 1.2). A complete log of the observations and the reduction procedure are presented in Paper I.

CTS J03.19, CTS J04.08, CTS J13.12, and CTS H34.06 were classified as NLS1's by us based on the appearance of their respective optical spectra. The criterion used in this classification is that the permitted lines be slightly broader than the forbidden lines, following the definition of Osterbrock & Pogge (1985). Mrk 1239, CTS R12.02 (=NGC 4748), and 1H 1934−063 are well-known NLS1 objects. For this reason, we consider that our sample is optically selected, in contrast to most NLS1's published in the literature, which are based on X-ray–selected objects. The luminosities of the galaxies are low to intermediate, and their radial velocities are not larger than 16,000 km s^{-1}. Figure 1 shows the spectra of the seven galaxies of the current study, already corrected for redshift.

Fe II emission, which is particularly strong in NLS1's, may alter the flux and width of Hβ+[O III] λλ4959, 5007. For this reason we have carefully removed the Fe II multiplets following the method described in Boroson & Green (1992). It consists of constructing a Fe II template by removing the lines that are not of Fe II from the spectrum of I Zw 1, a NLS1 galaxy widely known for the strength of the Fe II emission and the narrowness of its "broad lines." For this purpose, a high signal-to-noise ratio spectrum of I Zw 1 covering the spectral range 3500–6800 Å was taken in one of the observing runs. After isolating the Fe II emission, the template was broadened by convolving it with a Gaussian profile having a FWHM similar to that of the Hβ line and scaled to match the observed Fe II emission of the corresponding galaxy. Figure 2 shows the above procedure for 1H 1934−063 (*upper panel*), CTS R12.02 (*middle panel*), and Mrk 1239 (*lower panel*). Each panel shows the observed spectrum, the Fe II template, and the resulting spectrum after removing the Fe II emission. It can be seen that the most important Fe II features at both sides of Hβ have been cleanly removed leaving as a residual the true He II λ4686 line profile and, in Mrk 1239, the [Fe XIV] λ5302 line.

3. THE GAUSSIAN DESCRIPTION OF THE EMISSION-LINE PROFILES

3.1. *Results of Line Profile Fitting*

In order to characterize the emission-line profiles of the NLS1's we have assumed that they can be represented by a single or a combination of Gaussian profiles. The LINER routine (Pogge & Owen 1993), which is a χ^2 minimization algorithm that fits as many as eight Gaussians to a line profile, was used for this purpose.

As a first step we tried to fit the Hα emission line with a single Gaussian component. Hα is the strongest optical permitted line and is located in a spectral region with the highest S/N. It is therefore the best place to look for broad components to the permitted optical lines of NLS1's. The best fit obtained is shown in the left-hand panels of Figure 3. The thick line represents the synthetically calculated profile, and the dotted line represents the residuals of the fit. It is clear that this simplest representation cannot adjust adequately the wings of Hα, although its core is nicely fitted in most of the objects. We then tried to adjust a second Gaussian to Hα. The best solutions found are shown in the right-hand panels of the same figure. Now the residuals of the fit are quite similar to the noise level around Hα, implying that

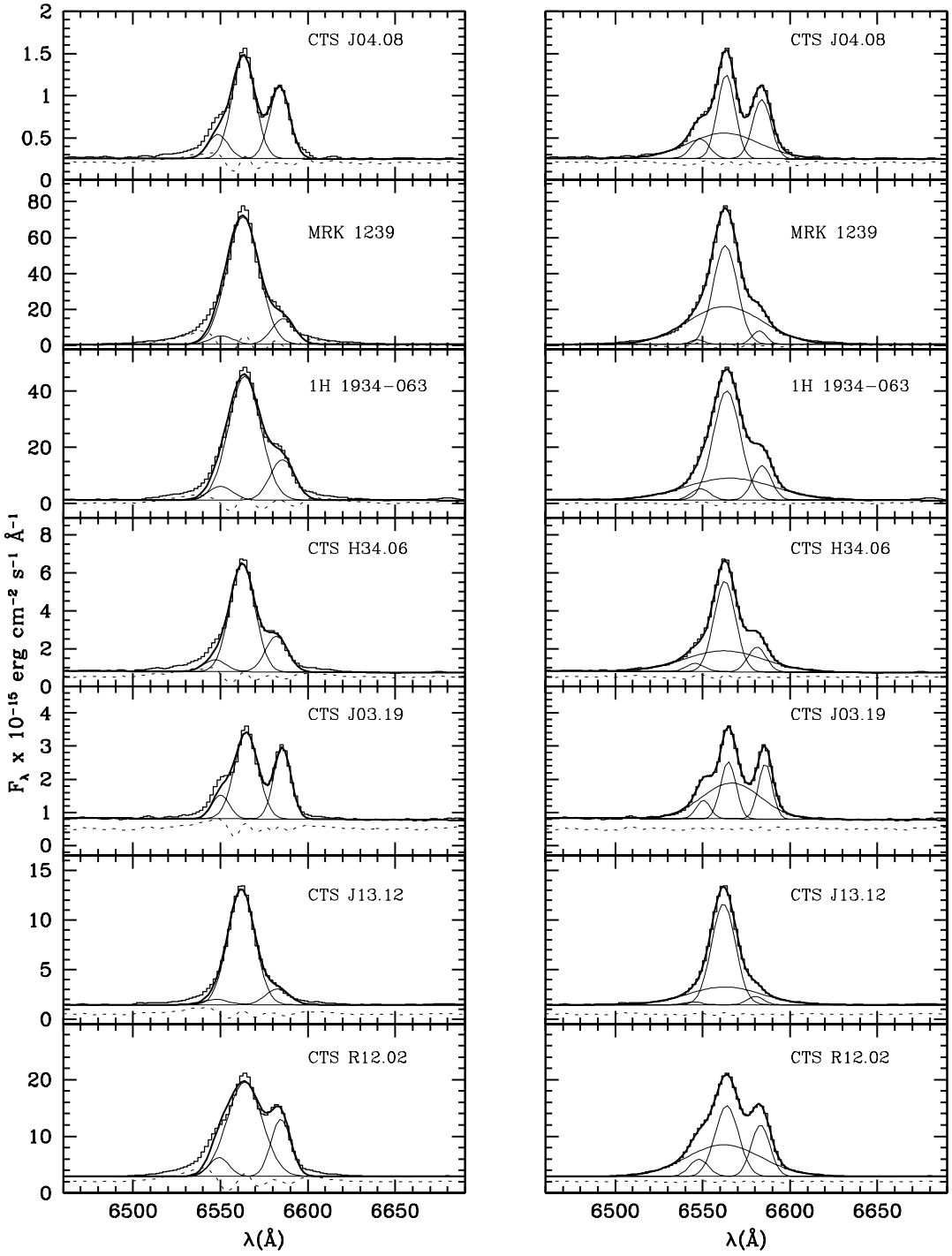

FIG. 3.—Gaussian fitting to the Hα + [N II] λλ6548, 6584 line profiles for the seven NLS1 galaxies of the sample. The left-hand panels show Hα fitted with a single component. The addition of a second, broader component to this line enhances the quality of the fit, as is shown in the right-hand panels. The histogram is the data, the thin lines represent the individual components and the underlying continuum, the dashed line represents the residuals of the fit, and the thicker line represents the synthetically calculated profile.

a narrow (FWHM $\sim$ 600 km s^{-1}) plus a broad component (FWHM $\sim$ 2500 km s^{-1}) give a convincingly better description of the observed profiles. In the above fits the only constraints applied were that [N II] λ6548 and [N II] λ6584 be of equal FWHM and that their flux ratio and wavelength separation be equal to their theoretical value (1:3 and 36 Å, respectively).

The same decomposition was applied to Hβ + [O III] λ4959, 5007. As for Hα, the fit of Hβ with a single Gaussian gives a poor representation of this line, and it was necessary to include an additional component to represent adequately the observed profile. Figure 4 shows the results of this decomposition. The residuals (*dashed line*) of the dual component fit (*right-hand panels*) are significantly improved

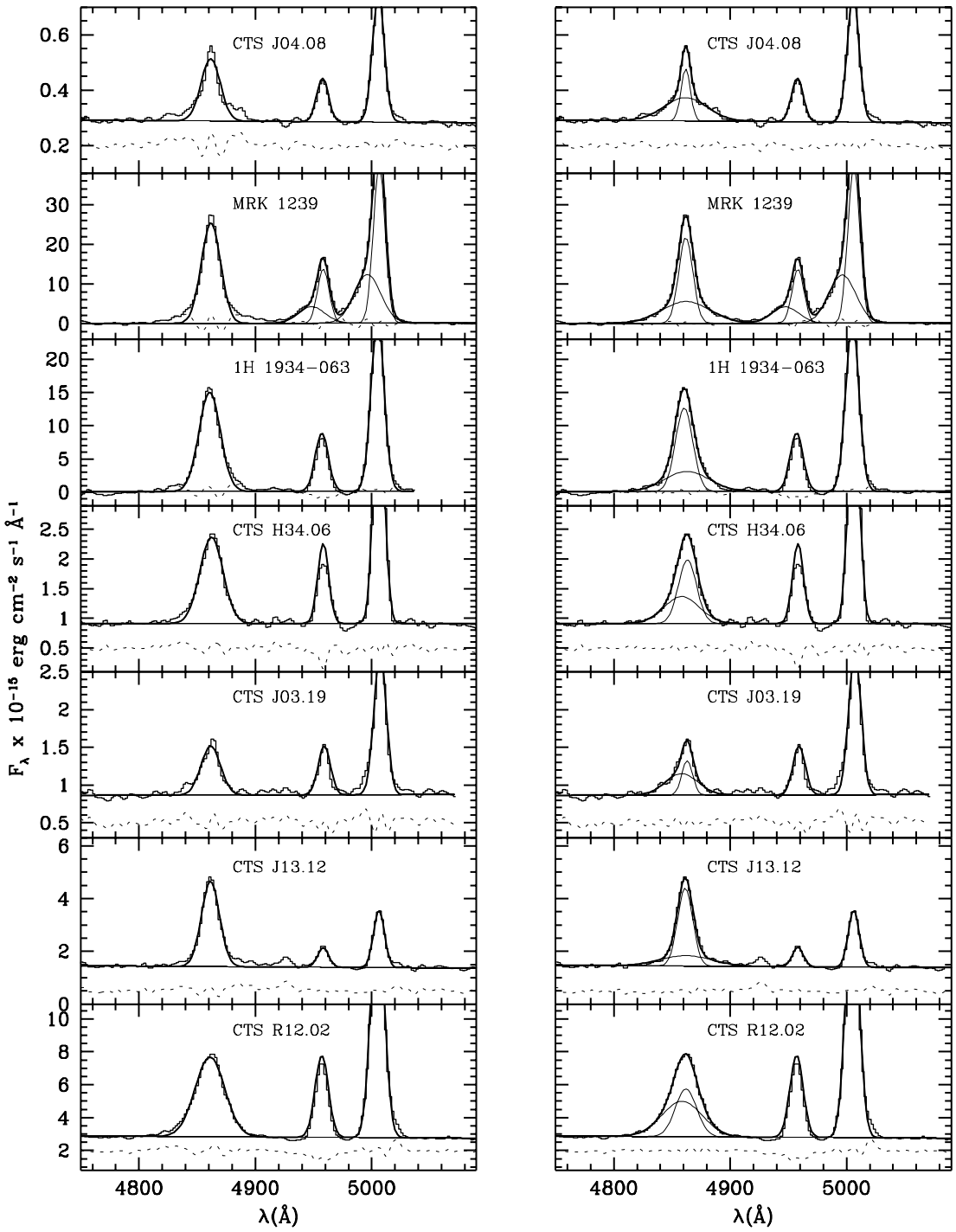

FIG. 4.—Same as Fig. 3 but to the Hβ + [O III] $\lambda\lambda$4959, 5007 lines

with respect to the fit with a single Gaussian (*left-hand panels*).

Columns (2)–(7) of Table 1 list the FWHM values (in km s^{-1}) of the emission lines measured from the Gaussian fitting. These values were obtained from the subtraction, in quadrature, of the observed FWHM and that of the instrumental profile, measured from the comparison lamp lines (FWHM $\sim$ 360 km s^{-1} at Hα). The flux ratio of the narrow to the broad component of Hβ for each galaxy is listed in column (8), and the [O III] λ5007 flux, relative to the narrow Hβ component, is in column (9). In all but one case (Mrk 1239), the center of the narrow components was coincident with the systemic velocity of the corresponding galaxy. Mrk 1239 presents a second blueshifted (with an outflow velocity of 600 km s^{-1} with respect to the nucleus) broader (FWHM $\sim$ 1580 km s^{-1}) component that is also present in Hα and Hβ (see Figs. 3 and 4) and that we associated to the NLR.

It is important to stress that the same result—i.e., a narrow component plus a broad one in the permitted lines of Hα and Hβ—would be obtained if instead of using the Gaussian decomposition technique we had employed the

TABLE 1

FWHM[a] AND FLUX LINE RATIOS IN NLS1's

	FWHM Hα		FWHM Hβ					
GALAXY	Narrow	Broad	Narrow	Broad	FWHM λ5007	FWHM λ6584	$F(H\beta_n/H\beta_b)$	$F(\lambda5007/H\beta_n)$
(1)	(2)	(3)	(4)	(5)	(6)	(7)	(8)	(9)
1H 1934−063.....	743	2703	926	2706	562	446	1.6	2.2
CTS H34.06.....	552	2401	972	2109	560	420	1.2	1.8
CTS J03.19.....	360	1766	560	1932	570	360	0.5	5.0
CTS J04.08.....	420	2152	560	2628	584	420	0.5	3.3
CTS J13.12.....	635	2212	762	3155	590	360	2.2	0.8
Mrk 1239.....	637	2278	683	2968	565	360	1.1	2.7
CTS R12.02.....	625	2272	1200	2434	583	448	0.7	3.4

[a] In units of km s^{-1}.

[O III] λ5007 line as a template representative of the NLR profiles. This test was applied to the Hβ line of the galaxy sample in order to see if the broad component found in the permitted lines using the Gaussian representation were not an artifact of the fitting procedure. For this purpose the [O III] λ5007 line was isolated and normalized to the peak intensity of the Hβ line to represent the maximum allowed Hβ contribution from the NLR to the observed profile. When subtracted, the residuals consist basically of a broad wing and a strong absorption coincident with the peak position of the template profile, such as shown in Figure 5 for the NLS1 galaxies 1H 1934−063, CTS R12.02, CTS J13.12, and Mrk 1239.

We interpret the broad wings as a clear evidence of the presence of a broad component similar to that observed in normal Seyfert 1 galaxies but with a smaller FWHM, supporting the results of Rodríguez-Pascual et al. (1997), Gonçalves, Véron, & Véron-Cetty (1999), and Nagao et al. (2000) who also report a broad component in the permitted lines of NLS1's. The absorption is interpreted as being due to an overestimation of the NLR component. Scaling the template profile in order to eliminate the absorption in the residuals leaves a pure broad component very similar in intensity and width to that found in the Gaussian decomposition (dashed line of Fig. 5). In fact, the values of FWHM and line fluxes obtained using this approach is essentially the same as those obtained formerly.

We conclude from the above test that the broad feature observed in Hβ and Hα is real, and it is interpreted here as the contribution from the BLR to the Hβ line.

Some authors (Moran, Halpern, & Helfand 1996; Gonçalves et al. 1999) have suggested that NLS1's have more nearly Lorentzian, rather than Gaussian, profiles, as evidenced by their cusped peaks and broad wings, mainly in Hβ and [O III] λ5007 lines and even in Hα. We have tested this hypothesis by fitting one-component Lorentzian profiles to the Balmer and adjacent lines. The best solution, plotted in Figure 6 for CTS R12.02, 1H 1934−063, and Mrk 1239, shows that this description does not provide a satisfactory fit to the emission lines. Very similar results were obtained for the other NLS1's of our sample. In all cases, the wings of the Lorentzians are more extended than the wings of the observed profiles. This effect is more pronounced in Hα (left-hand panels of Fig. 6) than in Hβ (right-hand panels), giving the apparent impression that this latter line is better fitted by a Lorentzian profile. We attribute this effect to the lower S/N of the Hβ region, which reduces the contrast of faint broad component wings relative to the narrow line. The poor fit obtained for the [O III] λλ4959, 5007 lines demonstrate that the Lorentzian profiles are unsuitable for representing the NLR profiles of NLS1's.

At this point it is important to note that the choice of the Gaussian profile as representative of the form of the observed emission lines was due to its simplicity and lack of physical reasons to adopt another particular form. We must be aware that the decomposition of the permitted lines into narrow and broad components, particularly in NLS1's, is a very uncertain task. As Evans (1988) noted, the fitting of symmetrical functional forms to the observed profiles may lead to the appearance of "components" in the center and wings of the lines but that, in certain circumstances, cannot bear any physical meaning. In addition, the observed profile can be the result of the superposition of many emitting regions located along the line of sight, each of them with a different intrinsic profile. For these reasons, one has to look with caution at the deblending into broad and narrow components obtained for the permitted lines. Nonetheless, the fact of having obtained similar results using two independent methods gives additional support to our interpretation.

3.2. *Meaning of the Narrow and Broad Components in NLS1's*

In the previous section we showed that the permitted lines of NLS1's can be decomposed into a narrow and a broad component, as is usually carried out in normal and intermediate Seyfert 1 galaxies. But what is the real meaning of this? A Gaussian representation as such, is only a mathematical way of fitting approximately the data. Additional evidence and a rationale are needed in order to identify each Gaussian component with physically different regions. Also, we must be aware that the number of Gaussian components adjusted to a given line basically depends on the spectral resolution and the S/N within the region of the fit.

Two important points call our attention regarding the values presented in Table 1. First, the FWHM of the "broad" components in Hα and Hβ are rather similar within the same galaxy and from object to object. Second, the FWHM of the narrow component of permitted lines is similar to that of the forbidden ([O III] and [N II]) lines. They are also larger than the width of the instrumental profile (FWHM $\sim$ 360 km s^{-1}).

It is generally accepted that the kinematics of the BLR clouds is largely dominated by the gravitational potential of the central black hole. The FWHM of the lines emitted in that region is a measure of the dispersion of velocities of the

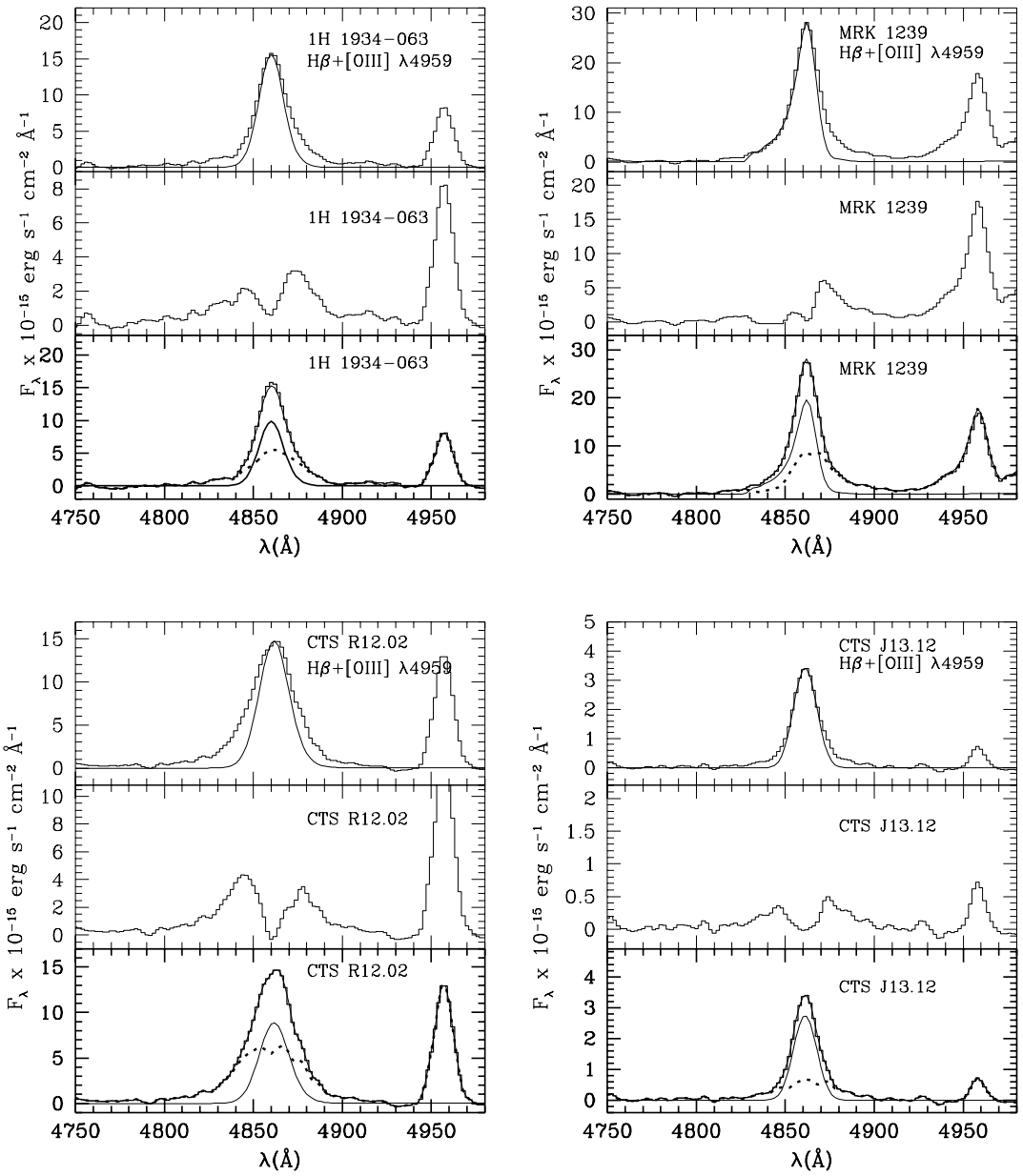

FIG. 5.—Example of the deblending procedure applied to the Hβ line using [O III] λ5007 as a template for the narrow components. For each galaxy, the top panel shows the template narrow line scaled to the peak intensity of the observed Hβ (*histogram*), and the middle panel shows the residuals after subtracting the template line. They consist of a broad wing, attributed to the presence of a second broader component of Hβ and a strong absorption due to an overestimation of the contribution of the narrow component. Reducing the strength of the narrow component so that no absorption is observed in the residuals (the bottom panel) leaves a pure broad component (*dashed line*) very similar to that found using the Gaussian decomposition.

emitting gas, along the observer's line of sight, which also represents the depth of the gravitational potential well in which the emitting clouds find themselves. For this reason, it is expected that lines formed in the same spatial region will have similar FWHM and emission-line profiles.

A similar argument can be applied to the narrow lines. However, the NLR is much more extended and located farther out from the central source (1–100 pc) so these clouds are immersed in a shallower gravitational potential dominated by the galaxy bulge.

Therefore, the consistency of the width and profile form of the broad components of Hα and Hβ and the similarity in width of the narrow permitted and forbidden lines, within the same galaxy, allow us to associate the narrow and broad Gaussian components of the permitted lines to the integrated line emission from the NLR and BLR, respectively.

A comparison of the FWHM of the narrow lines of our sample with those measured with a similar setup in normal Seyfert 1's (Cohen 1983; Stephens 1989; Puchnarewicz et al. 1997) shows that no differences seem to exist in the NLR kinematics between these two groups of galaxies.

The main difference lies in the BLR. The FWHM of the broad component is not only significantly smaller than that of the normal Seyfert 1's but also its relative contribution to the total flux of the line is greatly reduced in these objects. In column (8) of Table 1, we have listed the ratio of the flux

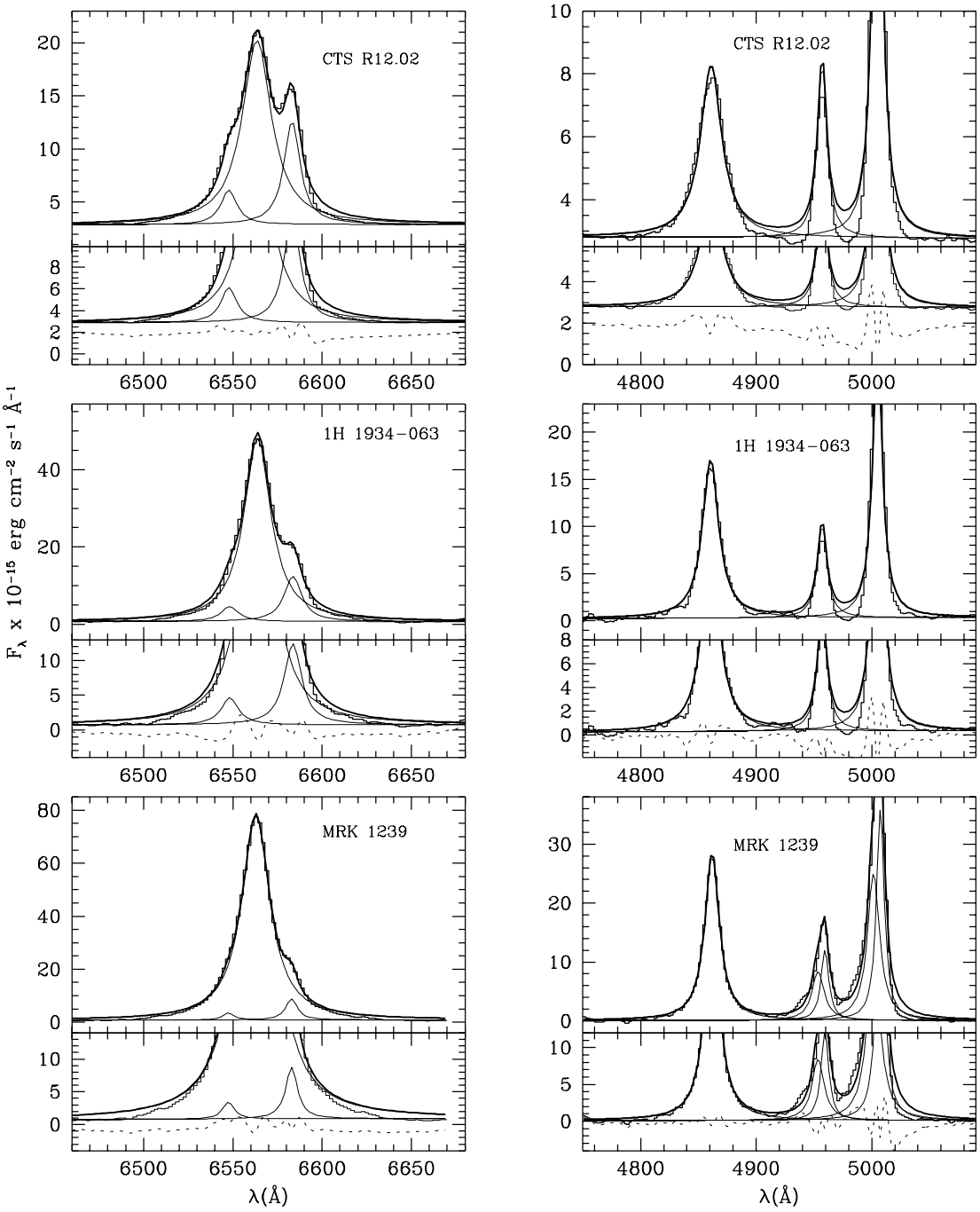

FIG. 6.—Fitting of Hα + [N II] (*left-hand panels*) and Hβ + [O III] λλ4959, 5007 (*right-hand panels*) for CTS R12.02 (*upper panel*), 1H 1934−063 (*middle panel*), and Mrk 1239 (*bottom panel*) with Lorentzian profiles. The histogram is the observed data, the thin lines represent the individual components and the underlying continuum, the thick line represents the resultant synthetic profile, and the dashed line represents the residuals of the fit. Note that in all cases the wings of the Lorentzians are more extended than the observed profiles.

associated to the narrow component to that of the broad one. It can be seen that on average, this ratio is very near unity, meaning that 50% of the total line flux is due to the narrow component. For comparison, this ratio is around 0.1 in typical Seyfert 1 galaxies.

The above results by themselves do not represent a major departure from our current picture of NLS1's. However, a significant difference emerges when we consider line ratios between the narrow component of Hβ and [O III] λ5007. In effect, since Osterbrock & Pogge (1995), and up to very recently (Leighly 1999), it has been assumed that the contribution in flux of the narrow component of Hβ to the NLR spectrum of a given object equals 10% of the flux of [O III] λ5007. This assumption is based on the fact that [O III] λ5007/Hβ is, on average, ∼10 in Seyfert 2 galaxies (Veilleux & Osterbrock 1987). Nonetheless, growing evidence of important differences between the NLR of Seyfert 1 and Seyfert 2 galaxies have appeared in the literature (Schmitt & Kinney 1996; Schmitt 1998; Paper I). In addition, NLS1's are recognized as a subclass within the realm of Seyfert 1's owing to their peculiar properties, making very unlikely that the above assumption really holds in these objects, as is

shown in column (9) of Table 1, which lists the [O III] λ5007/Hβ (narrow) ratio found from our decomposition of line profiles. These values also show that there is a wide intrinsic dispersion in the [O III] λ5007/Hβ ratio of NLS1's, ranging from 0.8 to 5.

Since the new values of the narrow [O III] λ5007/Hβ ratio are drawn from the decomposition into narrow and broad components of the Balmer lines, it is important to discuss the uncertainties inherent to the deblending process. Strictly speaking, one should be inclined to treat the flux associated to the narrow component of the permitted lines as a lower limit, being the actual flux between this value and that obtained from the total flux of the line. The latter option would be the case if no contribution from the BLR were present, as was initially suggested by Osterbrock & Pogge (1985) in order to explain the absence of broad permitted lines in NLS1's. Under the last circumstance, the resulting [O III] λ5007/Hβ ratio would be even smaller but would not change drastically. It would now fall into the interval 0.5–1.7, making the departure from the ratios found in normal Seyfert 1 galaxies even stronger.

One can argue that the deblending of the permitted lines overestimated the flux of the narrow Hβ component, making the [O III] λ5007/Hβ ratio appear smaller than it really does. That is, instead of being a lower limit, it represents an upper limit. Under this circumstance, the actual flux of the narrow Hβ would range between this upper limit and a small fraction of the total line flux. Physically, this is highly improbable, at least for two reasons. First, Hβ is emitted by every gas component, so the narrow Hβ cannot be narrower than the narrowest NLR line. This is in accord to the values of Table 1, in which the FWHM of Hβ is similar to that of [O III] λ5007 and of the same order of [N II] λ6584.

Second, let us suppose that the actual narrow Hβ flux corresponds to 50% of value obtained from the deblending process. With this in mind, the [O III] λ5007/Hβ ratio would now fall in the interval 1.6–10. But now a new problem will arise: the reddening measured from the Balmer decrement would be increased up to 0.7 mag. Such an increase in $E(B-V)$ would have a strong influence in the resulting emission-line spectrum. Probably new physical processes and ionization mechanisms should need to be invoked in order to explain the observed spectrum. In addition it would not be clear in which emitting region the remaining "narrow" flux would be produced. In the BLR? In the intermediate NLR?

In the following sections, additional evidence supporting the results obtained from the deblending process is given. Nonetheless, it is clear that a large spatial resolution, such as that obtained with the *HST*, is necessary in order to examine carefully the NLR of NLS1 galaxies.

4. MATTER-BOUNDED AND IONIZATION BOUNDED CLOUDS IN THE NLR OF NLS1'S

We have found that the NLR of NLS'1s are characterized by lower [O III] λ5007/Hβ ratios, more typical of some starburst or H II galaxies than of canonical Seyfert 1's or 2's. In addition, it was shown in Paper I that (1) NLS1's have intrinsically weak low ionization forbidden lines; (2) the dominant mechanism of the NLR emission is photoionization by a central source; and (3) a wide range of densities (10^3 cm^{-3} to 10^6 cm^{-3}) must exist in the NLR of these objects, with the larger densities associated to the inner NLR regions from which [O III] and the high ionization lines are emitted while the lowest values are associated to the [O I]– and [S II]–emitting regions.

A scenario that springs naturally from the above results invokes the presence of at least two types of clouds. A denser, inner set of high-excitation matter-bounded (MB) clouds is required to enhance the temperature-sensitive [O III] 4363 Å line relative to 5007 Å (due to collisional deexcitation) and also matter-bounded in order *not* to emit low-excitation lines (from low-ionization species such as O I, S II, N II, etc.). The MB component is where most of the [O III] emission and high-ionization lines such as He II, [Ne V], [Fe VII], and [Fe X] would be produced. To account for the lower excitation lines, it is necessary to consider a second component consisting of an outer, less dense set of ionization-bounded (IB) clouds, responsible for the production of low-ionization lines such as [O I], [N II], and [S II] (whose doublet ratio points to low densities) and some [O III] as well. These clouds must lie at a much larger distance in order that the ionization parameter be much smaller than the MB component as discussed in Rodríguez-Ardila, Pastoriza, & Maza (1998, hereafter RAPM). Our starting hypothesis is that the relative proportion of these two types of clouds combined with a suitable choice of the input ionizing continuum will reproduce the observed differences between the NLR of NLS1's and that of normal Seyfert 1 galaxies.

This dual-component model has been successfully applied before to account for the observed emission-line ratios of the NLR and extended narrow-line region of many Seyfert 1 and 2 galaxies (Binette, Wilson, & Storchi-Bergmann 1996; Binette et al. 1997; RAPM; Aita-Fraquelli, Storchi-Bergmann, & Binette 2000). Such a simple model is surely an oversimplification relative to the wide range in parameters needed to describe fully the NLR (to illustrate the complexity of the problem, see Moore & Cohen 1996, Ferguson et al. 1997, and Komossa & Schulz 1997). However, in the absence of sufficient observational constraints on all possible models and geometries of the NLR, it appears to us to be the simplest means for taking into account the particular emission-line signature reported in RAPM, that is a high-density, high-excitation spectrum observed in conjunction with the presence of low-density, low-excitation lines.

4.1. *The Photoionization Models*

In this section we test whether the simplified dual-component MB-IB description can satisfactorily account for the anomalous line ratios observed in NLS1's. We are particularly interested in determining which kind of spectral energy distribution (SED) observed in AGNs can best produce a [O III] λ5007/Hβ ratio in the range 1–5 and the strongest optical emission lines, using similar physical parameters to those employed to model the NLR of normal Seyfert 1 galaxies.

Although there is no direct way to determine the intrinsic shape of the ionizing continuum in the EUV domain, recent work by Zheng et al. (1997) and Laor et al. (1997) show that the ionizing continuum, from the Lyman limit to soft X-ray energies, may be characterized by a power law of index $\alpha \sim -2$. This result was derived from QSOs of intermediate redshifts but may be extended to lower luminosity AGNs such as Seyfert 1 galaxies. Korista, Ferland, & Baldwin (1997) suggest flatter indices $\alpha \sim -1.5$, which have been

used by Binette et al. (1996) and RAPM, for instance, in their modeling of Seyfert 1 objects. Meanwhile, *ROSAT* observations of NLS1's show that the soft X-ray photon index is systematically steeper than that of Seyfert 1 galaxies with broad optical lines (BBF96; Foster & Halpern 1996; Laor et al. 1997).

For of the above reasons, we generated sequences of models assuming a SED of broken power laws of the form $F_\nu = K\nu^\alpha$, where

$$\alpha = -1.4,\ 13.6\ \text{eV} \leq h\nu \leq 1300\ \text{eV};$$
$$\alpha = -0.4,\ h\nu \geq 1300\ \text{eV} \quad (1)$$

$$\alpha = -2.2,\ 13.6\ \text{eV} \leq h\nu \leq 2000\ \text{eV};$$
$$\alpha = -1.1,\ h\nu \geq 2000\ \text{eV}\ . \quad (2)$$

Equation (1) (SED 1) corresponds to the fit made by Kraemer et al. (1998) to the observed SED of the Seyfert 1 galaxy NGC 5548. Equation (2) (SED 2) uses the median values of the spectral indices found from *ROSAT* and ASCA data for NLS1's (Leighly 1999).

For each SED, the $A_{\rm M/I}$ parameter, which characterizes the relative proportion of MB and IB clouds, was varied from 0.04 to 11. Density estimates of the NLR of NLS1's based on density and temperature line ratios (cf. Paper I) show that MB clouds should have $n_e \sim 10^6$ cm^{-3}, while in IB clouds, $n_e \sim 10^3$ cm^{-3}. The ionization parameter $U_{\rm MB}$ at the illuminated face of the MB clouds was initially set to $10^{-1.5}$, following estimates by RAPM and Kraemer et al. (1998, 1999) for normal Seyfert 1 galaxies.

The multipurpose code MAPPINGS Ic (Ferruit et al. 1997) was used to compute the dual-component photoionization models. Plane-parallel geometry was assumed given the relatively large distance of the ionized clouds from the central source compared to the geometrical depth of the clouds. The gas is assumed to be atomic and the gas abundances solar. In order to let the inner set of clouds be matter-bounded, a fraction $F_{\rm MB}$ of the input ionizing continuum is left to escape from the back of the clouds. This fraction was initially set to $\sim$60% (the value used in Ferruit et al. 1997) but was allowed to increase substantially for the models making use of the steep SED. This was necessary in order to keep a high value of the He II/Hβ ratio emitted by the MB component, an essential ingredient of the dual-component models. The "filtered" continuum is later used to ionize the IB clouds farther out (which do not emit any He II). The IB clouds integration is stopped when the electron temperature falls below 5000 K. Dust is considered to be mixed with the ionized gas, and the code includes heating by dust photoionization. The dust content of the photoionized plasma is described by the quantity μ, which is the dust-to-gas ratio of the plasma expressed in units of the solar neighborhood dust-to-gas ratio ($\mu = 1$). In this work we use a constant $\mu = 0.015$, which has a negligible effect on line transfer and on the gas heating.

Figure 7 shows the predicted [O III] λ5007, He II λ4686, [O I] λ6300, and [O III] λ4363, relative to Hβ as function of the relative proportion of MB and IB clouds, $A_{\rm M/I}$. The solid line corresponds to the predictions of SED 1, and the dashed line corresponds to the ratios obtained with SED 2. In order to compare the output with the observations, we have plotted the dereddened observed ratios for the NLS1 galaxies CTS H34.06 (*filled triangle*), 1H 1934−063 (*filled square*), CTS R12.02 (*filled circle*), and Mrk 1239 (*open square*) as taken from Paper I. NGC 5548 was chosen as representative of the normal Seyfert 1 galaxies. Its dereddened ratios were taken from Kraemer et al. (1998) and are shown as filled diamonds. Table 2 lists the predictions of the best-fit model for the most important optical lines observed in each galaxy and the parameters of the corresponding model.

A close inspection of Figure 7 and the values of Table 2 allows us to say that our approach is successful at reproducing the observed ratios overall. The fact of being able to predict simultaneously and accurately the [O III] λ5007/Hβ and He II λ4686/Hβ ratios for the NLS1 galaxies and NCG 5548 indicates that the general distribution of ionizing photons at least in the range 13.6–100 eV is correct. Since the model parameters were rather similar for the two SEDs, the results provide a strong support to the idea that the NLR of NLS1's and Seyfert 1's have similar physical

TABLE 2

LINE RATIOS (RELATIVE TO Hβ) FROM MODELS AND OBSERVATIONS

	CTS H34.06		1H 1934−063		CTS R12.02		Mrk 1239		NGC 5548	
LINE	Model	Obs.	Model	Obs.	Model	Obs.	Model	Obs.	Model	Obs.
[Ne III] λ3869.....	0.36	0.21±0.07	0.44	0.27±0.07	0.67	0.45±0.07	0.54	0.18±0.02	1.56	1.32±0.18
[O III] λ4363.....	0.13	0.20±0.04	0.18	0.10±0.04	0.34	0.29±0.06	0.26	0.25±0.04	1.25	0.77±0.11
He II λ4686.....	0.08	0.06±0.03	0.11	0.13±0.04	0.20	0.21±0.03	0.15	0.20±0.04	0.29	0.23±0.05
[O III] λ5007.....	1.72	1.79±0.52	2.14	1.95±0.40	3.40	3.40±0.44	2.69	2.69±0.60	7.87	8.07±0.88
He I λ5875	0.14	0.15±0.02	0.12	0.22±0.05	0.10	0.15±0.06	0.13	0.13±0.02	0.11	0.21±0.05
[O I] λ6300	0.25	0.14±0.04	0.24	0.10±0.02	0.20	0.13±0.06	0.22	0.10±0.03	0.42	0.31±0.07
[N II] λ6584	2.39	0.72±0.10	2.27	0.69±0.13	1.91	1.75±0.18	2.11	0.28±0.03	1.82	0.76±0.15
[S II] λ6725[a]	0.95	0.47±0.12	0.90	0.33±0.08	0.75	0.72±0.06	0.83	0.16±0.04	1.28	0.66±0.10
[S III] λ9525	1.28	0.20±0.08	1.22	0.50±0.10	1.04	0.60±0.15	1.14	0.10±0.04	0.75	0.68±0.13
$A_{\rm M/I}$	1.0		1.5		2.2		3.3		1.5	
$U_{\rm MB}$	$10^{-1.4}$		$10^{-1.4}$		$10^{-1.4}$		$10^{-1.4}$		$10^{-1.5}$	
$n_{\rm H,MB}$ (cm^{-3})	10^6		10^6		10^6		10^6		10^6	
SED.....	(1)		(2)		(2)		(2)		(2)	
$F_{\rm MB}$ (%).....	85		85		85		85		54	

[a] Sum of fluxes of [S II] $\lambda\lambda$6717, 6731.

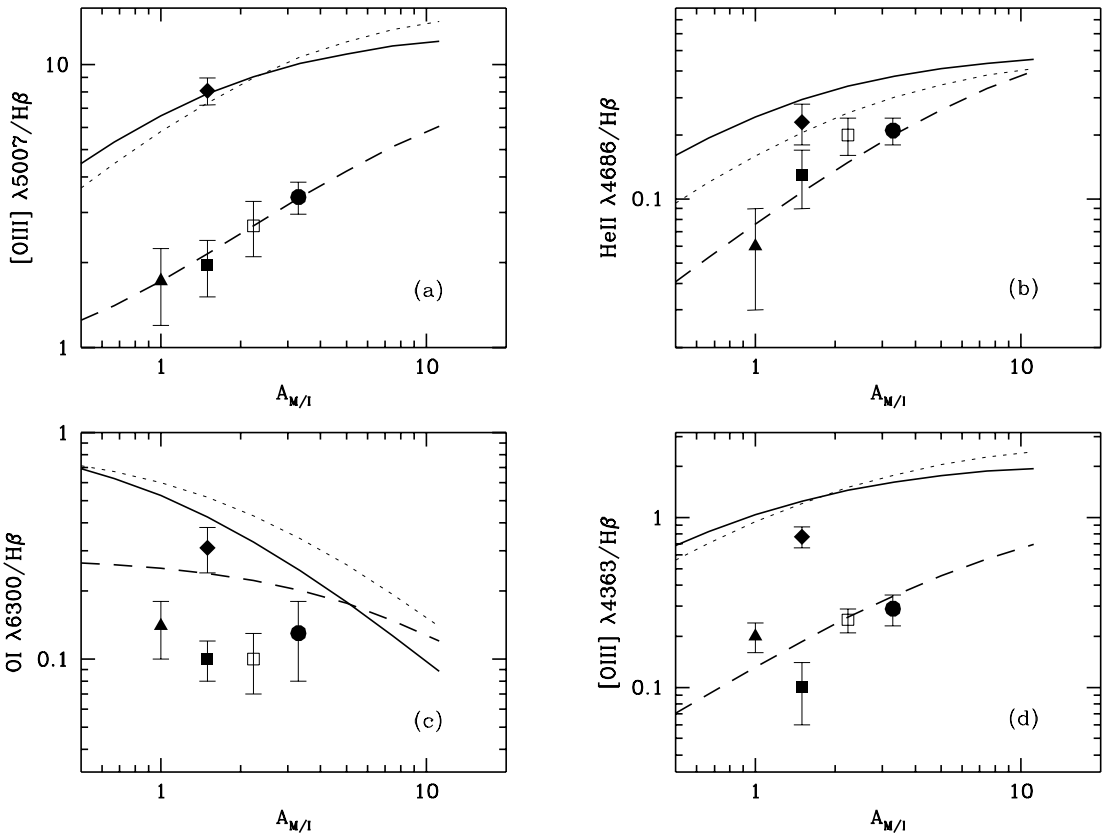

FIG. 7.—Theoretical emission-line ratios as function of the relative proportion of MB and IB clouds, $A_{M/I}$. The solid line corresponds to the predicted narrow line ratios under SED 1 and the long-dashed line to the output of SED 2 (see text for further details). The short-dashed line shows the effects on the line ratios by the inclusion of UV-absorbing material (WA with $U_{WA} = 0.01$) between the BLR and NLR. The filled triangle, filled square, filled circle, and open square are the observed dereddened line ratios of the NLS1 galaxies CTS H34.06, 1H 1934−093, CTS R12.02, and Mrk 1239, respectively. The diamond corresponds to the normal Seyfert 1 galaxy NCG 5548.

properties in terms of density, chemical abundance, ionization parameter, and distance to the central source. The most probable cause of the observed spectral differences can be related to the variation in steepness of their ionizing continuum.

The largest discrepancies between models and observations, for some of the galaxies, are in low-excitation lines ratios such as [O I] λ6300/Hβ, [S II] $\lambda\lambda$6717, 6731/Hβ, and [N II] λ6584/Hβ. These are overpredicted by a factor of 2 in CTS H34.06, 1H 1034−063, and Mrk 1239.

This systematic overprediction, nonetheless, might provide helpful constraints to the physical conditions of the IB clouds and the nature of the central ionizing source. In effect, it is well known that the low-ionization lines of AGNs are produced by the flux of high-energy EUV photons in the range 300–900 eV (cf. Fig. 1 in Binette et al. 1997) which penetrate deep into the NLR gas. If these photons are not allowed to reach this region, intrinsically weaker low-ionization lines will be emitted. A possible candidate for this shielding might plausibly be a high-ionization warm absorber (hereafter WA), located near the BLR. Evidences for the existence of such an absorbing material have been found in several NLS1's, particularly in those with high polarization (Leighly et al. 1997). Mrk 1239, the NLS1 with the largest discrepancies between the predicted and observed low-ionization lines (cf. Table 2), is widely known for being highly polarized (Goodrich 1989) and for showing WA spectral features (Leighly et al. 1997; Grupe et al. 1998). In contrast, CTS R12.02 (=NGC 4748) shows one of the lowest percentage of polarization (0.12% against 2.89% for Mrk 1239) according to Goodrich (1989) and presents here the best agreement between the model and the observed line ratios, even in the low-ionization lines. No report about X-ray WA features are found in the literature for this galaxy.

Although polarization data for the remaining NLS1's are not available at present, the case of Mrk 1239 can be taken as a good evidence for attenuation of the hard X-ray continuum and its influence on the NLR emitted spectrum. We discard the possibility of higher densities for the IB clouds since the derived value using the [S II] $\lambda\lambda$6717/6731 ratio in the galaxies are near 10^3 cm^{-3}.

Although a finer tuning of the parameters might improve the agreement between the observations and the model predictions for the objects studied here, this is unwarranted considering the simplicity of the approach taken. What is important to note is that the same initial set of physical conditions (albeit different SED) derived independently for normal Seyfert 1's are also valid to reproduce to a first approximation the emission-line ratios observed in NLS1's.

5. NEW EMISSION-LINE RATIOS FOR THE NLR OF NLS1'S

As was discussed in the Introduction and § 3.2, one of the main purposes of this paper is to review the current assumption that the NLR contributes Hβ with 0.1 times the flux of [O III] λ5007, implying a universal constant [O III] λ5007/

Hβ ratio of 10 (Osterbrock & Pogge 1985; Leighly 1999). This assumption is usually made because of the difficulty in deblending the narrow and broad components of the permitted lines in these objects and is based on trends observed in narrow emission lines of Seyfert 2's and intermediate Seyfert 1 galaxies. According to the results obtained in § 3 the NLR of NLS1's contributes 50% of the total Hβ emission. This has important implications for the intrinsic ratios of the narrow lines. For instance, [O III] λ5007/Hβ (narrow) now falls in the interval 1–5 since narrow Hβ sees its flux increased by up to ten times its previously assumed value.

If we had (erroneously) assumed that in NLS1's the [O III] λ5007/Hβ (narrow) ratio took the canonical value of 10 of normal Seyfert galaxies, we would have inferred a spectral index $\leq \alpha \sim -1.4$ to describe the EUV–to–soft X-ray SED since such hardness is favored when attempting to reproduce a high ratio. The *ROSAT* observations, however, show that the soft X-ray spectra from NLS1's is systematically steeper ($\alpha \sim -2$ or smaller) than those from Seyfert 1 galaxies with broad optical lines. In addition, Table 2 shows that photoionization models with $\alpha \sim -2.2$ always provide [O III] λ5007/Hβ ratios smaller than 7 under the initial set of conditions assumed. This result is therefore fully consistent with our findings of a much lower ratio in NLS1's than in normal Seyfert galaxies. Beside, much lower NLR densities ($n_B \sim 10^5$ cm^{-3}) would have been required to get [O III] λ5007/Hβ around 10 using SED 2. Such low densities would be discrepant with the higher ones determined in Paper I and from other authors (Osterbrock & Pogge 1985).

One possibility is that the continuum in the 13.6–200 eV region that photoionizes the NLR of NLS1's is similar to that of NGC 5548 (SED 1) but that it is modified before reaching the NLR gas by intervening material located between the BLR and NLR. Kraemer et al. (1999) explored, for instance, the effects of UV-absorbing material on the shape of the continuum radiation emitted from the AGN and on the relative strengths of the ensuing emission lines formed in the NLR of Seyfert 1 galaxies exposed to this emerging continuum distribution. Their results indicated that a low-ionization UV absorber with a large covering factor can indeed modify the intrinsic EUV continuum of the central source and produce significative variations in the NLR emission spectrum of the AGN compared to that produced by the unattenuated continuum. Nonetheless, among the various types of warm absorbers tested, no model could reproduce a low [O III] λ5007/Hβ ratio. It should be mentioned that they assumed the NLR gas to be uniformly radiation-bounded unlike the models presented here, which consist of a combination of MB and IB components.

We consider it worthwhile to test whether the inclusion of a low-ionization WA with similar characteristics to that of Kraemer et al. (1999) and exposed to SED 1 might explain the strongest (narrow) line ratios observed in NLS1's. In this picture, differences in [O III] λ5007/Hβ, for example, would be caused by the effects of the intervening WA rather than by changes in steepness of the intrinsic EUV–soft X-ray continuum, as was suggested in the preceding section. Results are presented in Figure 7, where the short-dashed line shows the predicted line ratios for a NLR with the same physical parameters as employed in modeling NCG 5548 but photoionized by the continuum leaking from a WA with $U_{\rm WA} = 0.01$, $n_{\rm H} = 1 \times 10^7$ cm^{-3}, solar abundance, and thickness $N_{\rm H} = 10^{20}$ cm^{-2}. The intrinsic SED incident on the WA was SED 1.

Comparison of these results with those of the unabsorbed model (*solid line*) allows us to say that the variations of the emission-line ratios introduced by an intervening low-ionization WA are relatively minor and clearly insufficient for explaining the differences in line ratios observed between NLS1's and normal Seyfert 1 galaxies. On the other hand, models with $U_{\rm WA} < 10^{-2.5}$ are found to alter the incident EUV–to–soft X-ray distribution in such a way that few photons are left to ionize the NLR as in Kraemer et al. (1999). It can be seen that the [O III] λ5007/Hβ ratio does not change significantly relative to the unabsorbed model. In either cases, low-ionization lines such as [O I] λ6300 (Fig. 7*c*) see their ratios increased relative to Hβ. The same trend is observed for [N II] λ6584 and [S II] $\lambda\lambda$6717, 6731. We recall from the previous section that these lines were already overpredicted. The lower the ionization degree of the WA, the larger this effect. This is clearly understood if we consider that the net effect of a low-ionization WA is to modify the EUV distribution, while the hard EUV portion is left unaltered. Since low-ionization lines are produced by the harder EUV radiation, they are now augmented owing to the reduction of ionizing photons that produce the Balmer and He II λ4686 lines.

We therefore conclude that a low-ionization WA, if it exists in NLS1's, cannot explain the low [O III] λ5007/Hβ ratio observed in these objects.

6. CONCLUSIONS

We have analyzed long-slit spectral data of a sample composed of seven NLS1 galaxies. A decomposition of the Hα and Hβ emission-line profiles into Gaussian components allowed us to separate the flux contribution of the NLR from the total flux of the line. Our results show that, on average, 50% of the total Hβ flux is due to emission from the NLR. Using the [O III] λ5007 line profile as a template for the narrow lines in order to subtract this contribution in the permitted lines gives very similar results to those obtained through the Gaussian decomposition. This confirms the presence of a broad component in the permitted lines.

The FWHM of the broad components of Hα and Hβ in the NLS1's studied here seems to be rather uniform within the same galaxy after comparing Hα and Hβ and throughout the sample (2250 km s^{-1} and 2560 km s^{-1} for Hα and Hβ, respectively). No evidence of Lorentzian profiles was observed either in the narrow or the broad lines. The narrow components of Hα and Hβ present FWHM comparable to those of the forbidden lines that are typical of the NLR in any Seyfert galaxy.

The resulting [O III] λ5007/Hβ ratios fall in the interval 1–5, significantly lower than the value currently assumed ($\sim$10). This entails that the emission-line ratios from the NLR are different in NLS1's from those observed in normal and intermediate Syfert 1 galaxies.

We test photoionization models that consider a NLR composed of a combination of matter-bounded clouds and ionization-bounded clouds. The former, with typical densities $\sim 10^6$ cm^{-3} and photoionized by the intrinsic continuum from the central source, are responsible for the emission of most of the [O III] and high-ionization lines. This component should be located in the inner regions of the NLR. The latter, located farther out than the MB clouds

and characterized by a lower density ($n_e \sim 10^3$ cm^{-3}), are photoionized by the continuum filtered from the MB clouds and emits most of the low-ionization lines. Assuming similar physical parameters in the NLR of NLS1's and normal Seyfert 1 galaxies, we show that the observed differences in emission-line ratios between these two groups of galaxies can be explained in terms of differences in the form of the input ionizing spectra. NLS1 ratios are better reproduced with a steep power-law continuum, with spectral index $\alpha < -2$, while flatter spectral indices ($\alpha \sim -1.5$) match the observed line ratios in normal Seyfert 1 galaxies. This scenario reproduces with very good agreement the line ratios of NLS1's. It is furthermore consistent with *ROSAT* observations of NLS1's, which show that these objects are characterized by steeper power-law indices than those of Seyfert 1 galaxies with broad optical lines. Our modeling therefore supports the view that the NLR is directly photoionized by the unaltered SED distribution emitted by the central engine.

A. R. A. gratefully acknowledges the staff of the CASLEO Observatory for instrumental and observing assistance. This research has made use of the NASA/IPAC Extragalactic Database (NED) which is operated by the Jet Propulsion Laboratory, California Institute of Technology, under contract with the National Aeronautics and Space Administration. The work of Luc Binette was supported by the CONACyT grant 27546-E, and the work of A. R. A. and M. G. P. was supported by the PRONEX/FINEP grant 76.97.1003.00

REFERENCES

Aita-Fraquelli, H., Storchi-Bergmann, T., & Binette, L. 2000, ApJ, 532, 867
Binette, L., Wilson, A. S., Raga, A., & Storchi-Bergmann, T. 1997, A&A, 327, 909
Binette, L., Wilson, A., & Storchi-Bergmann, T. 1996, A&A, 312, 365
Boller, Th., Brandt, W. N., & Fink, H. 1996, A&A, 305, 53 (BBF96)
Boroson, T. A., & Green, R. F. 1992, ApJS, 80, 109
Cohen, R. D. 1983, ApJ, 273, 489
Evans, I. N. 1988, ApJS, 67, 373
Ferguson, J. W., Korista, K., Baldwin, J. A., & Ferland, G. J. 1997, ApJ, 487, 122
Ferruit, P., Binette, L., Sutherland, R. S., & Pécontal, E. 1997, A&A, 322, 73
Foster, K., & Halpern, J. P. 1996, ApJ, 468, 565
Gonçalves, A. C., Véron-Cetty, M.-P., & Véron, P. 1999, A&AS, 135, 437
Goodrich, R. W. 1989, ApJ, 342, 224
Grupe, D., Wills, B. J., Wills, D., & Beuermann, K. 1998, A&A, 333, 827
Komossa, S., & Schulz, H. 1997, A&A, 323, 31
Korista, K. T., Ferland, G. J., & Baldwin, J. A. 1997, ApJ, 487, 555
Koski, A. T. 1978, ApJ, 223, 56
Kraemer, S. B., Crenshaw, D. M., Filippenko, A. V., & Peterson, B. M. 1998, ApJ, 499, 719
Kraemer, S. B., Turner, T. J., Crenshaw, D. M., & George, I. M. 1999, ApJ, 519, 69
Laor, A., Fiore, F., Elvis, M., Wilkes, B. J., & McDowell, J. C. 1997, ApJ, 477, 93
Leighly, K. M. 1999, ApJS, 125, 317
Leighly, K. M., Kay, L. E., Wills, B. J., Wills, D., & Grupe, D. 1997, ApJ, 489, 137
Moore, D., & Cohen, R. D. 1996, ApJ, 470, 301
Moran, E. C., Halpern, J. P., & Helfand, D. J. 1996, ApJS, 106, 341
Nagao, T., Murayama, T., Taniguchi, Y., & Yoshida, M. 2000, AJ, 119, 1691
Osterbrock, D. E., & Pogge, R. W. 1985, ApJ, 297, 166
Pogge, R. W., & Owen, J. M. 1993, OSU Internal Report 93-01
Puchnarewicz, E. M., et al. 1997, MNRAS, 291, 177
Rodríguez-Ardila, A., Pastoriza, M. G., & Donzelli, C. J. 2000, ApJS, 126, 63
Rodríguez-Ardila, A., Pastoriza, M. G., & Maza, J. 1998, ApJ, 494, 202 (RAPM)
Rodríguez-Pascual, P. M., Mas-Hesse, J. M., & Santos-Lléo, M. 1997, A&A, 327, 72
Schmitt, H. R. 1998, ApJ, 506, 647
Schmitt, H. R., & Kinney, A. L. 1996, ApJ, 463, 498
Stephens, S. A. 1989, AJ, 97, 10
Ulvestad, J. S., Antonucci, R. R. J., & Goodrich, R. W. 1985, AJ, 109, 81
Veilleux, S., & Osterbrock, D. E. 1987, ApJS, 63, 295
Zheng, W., Kriss, G. A., Telfer, R. C., Grimes, J. P., & Davidsen, A. F. 1997, ApJ, 475, 469